Radiation-induced defects in solar cell materials

J.C. Bourgoin*, N. de Angelis

*Laboratoire des Milieux Désordonnés et Hétérogènes, Université P. et M. Curie, CNRS, UMR 7603, Tour 22,
Casier 86, 4 place Jussieu, 75252 Paris Cedex 05, France*

Abstract

We review the knowledge and understanding of proton and electron irradiation-induced defects in Si, GaAs and GaInP. We describe their nature, evaluate their introduction rates, give the electronic characteristics of the defects which play the role of recombination centers and of those which play the role of compensating centers. We then briefly describe the techniques which allow to determine these characteristics and to differentiate recombination centers and compensating centers among all the created defects. Finally, we develop and illustrate the role these specific defects play on the current generated by a solar cell. © 2001 Elsevier Science B.V. All rights reserved.

Keywords: Defects; Si; GaAs; GaInP; Irradiation

1. Introduction

Many different semiconductor materials can potentially be used to make solar cells. However, when a high efficiency is required, the choice of the material becomes restricted to Si, GaAs, InP and GaInP alloys and related heterostructures. This is because only these materials can be grown with a good crystalline quality, a controlled impurity content and a large enough lifetime. Si, GaAs and GaInP possess also the overwhelming advantage of a sufficiently well-mastered technology.

The study of radiation induced degradation of solar cells, being in practice only interesting for space applications, is of course restricted to the high-efficiency materials. For this reason, in this communication we only consider the defects induced in Si, GaAs and GaInP currently used to make space solar cells. For this we recall, in

*Corresponding author. Tel.: + 33-1-44-27-79-98; fax: + 33-1-4427-7998.
E-mail address: bourgoin@ccr.jussieu.fr (J.C. Bourgoin).

Section 1, the mechanism of defect production in these materials by electron and proton irradiations. We then describe, in Section 2, the knowledge which has been acquired on the introduced defects, i.e. their nature and their electrical characteristics, focusing on the defects which play a role in the degradation, namely the defects acting as recombination centers and those acting as compensating centers. Section 3 deals with the techniques allowing to select such defects among many others and to get their electrical characteristics. In Section 4, we explain the role each specific type of defect plays on the behaviour of a solar cell. Finally, we illustrate these considerations by describing the degradation of Si, GaAs and GaInP cells, submitted to electron irradiation. We show how the parameters necessary to predict a degradation can be extracted from the fluence dependence of the short-circuit current.

2. Mechanism of defect production

An energetic proton which enters in a material loses first its energy in electronic collisions. When its energy becomes low enough, it then interacts with nuclei and produces atomic displacements. Hence, the incident energy E of the proton determines the depth R_p (projected range) at which these displacements are produced. But the average energy, T, dissipated into atomic collisions and, consequently, the number of displacements is practically E independent. The average number of displacements v per proton is $v = T/2T_d$ where T_d, is the so-called threshold energy, is the minimum energy which should be transmitted to an atom to induce its displacement. In semiconductors, T_d is of the order of 20 eV [1]. So, for instance, in Si where $T = 10^2$ eV, $v = 5$. The displacements are concentrated in the volume of a cascade, of the order of $10^{-14} - 10^{-12}$ cm^{-3}, providing a local concentration of displacements C ranging from 10^{12} to 10^{14} cm^{-3}.

In case of a monodirectional irradiation, all displacements pile up in a layer located at the depth R_p and the defects resulting from the displacements, located within this layer, can be in large concentration. This is usually revealed by the interactions between defects, giving rise to a broad distribution of their electronic characteristics. However, in space, the irradiation is isotropic and the displacements are homogeneously distributed in depth, up to the maximum depth R_p. The defect concentration, resulting from an irradiation with a fluence φ, is then $v\varphi/R_p$, i.e. the defect introduction rate is v/R_p.

Electron irradiation produces also a uniform distribution of displacements. Typically, electrons in the range 0.1 to several MeV produce one to two displacements with an introduction rate of the order of 1 cm^{-1} at 1 MeV [2]. Typically, a fluence of 10^{16} cm^{-2} is necessary to create a uniform distribution of displacements with a 10^{16} cm^{-3} concentration.

Thus both types of irradiations, with electrons or isotropic protons, result essentially in uniform distributions of displacements, and hence of defects [3], because the local concentration of displacements in the volume of a cascade produced by a proton remains small enough (10^{13} cm^{-3} for 1 MeV protons) so that interaction between defects is negligible.

3. Nature and properties of the defects

The defects produced by irradiation at room temperature can be of different nature depending on the material. They are primary defects in GaAs, i.e. the defects resulting from direct atomic displacements (vacancies and interstitials) thermally stable at 300 K. In Si, they are secondary defects resulting from the interaction of the primary defects with impurities or with each others, because the primary defects are mobile well below 300 K. In GaInP, not enough information is yet available to make any firm conclusion on the nature of the defects present at 300 K.

In this section, we describe the characteristics of these defects, focusing on those which play the role of recombination centers and of compensating centers.

3.1. GaAs

Systematic studies (for a review, see Ref. [4]) by deep level transient spectroscopy (DLTS) performed in n-type GaAs have shown that the defects introduced in n-type GaAs are different configurations of vacancy interstitial pairs in the As sublattice [5,6]. This picture seems to be valid also for p-type GaAs [7]. Annihilation of the pairs occurs around 300°C through the mobility of As interstitials, as demonstrated by the annealing kinetics in low-temperature grown GaAs [8].

Among all the detected defects, the defect labelled E4, whose level is located very near midgap (at 0.76 eV below the conduction band) should be the lifetime killer. Its introduction rate is $v \sim 0.1 \, \text{cm}^{-1}$ and its electron cross section $\sigma_n \sim 3 \times 10^{-14} \, \text{cm}^2$ [4]. It probably corresponds to the H_3 hole trap observed in p-type materials located at 0.71 eV above the valence band [7]. It is possible that this defect is in fact the EL2 defect, a defect associated with the As antisite (for a review on the properties of this defect, see Ref. [9]). Indeed, it has been argued that this last defect is induced by proton or electron irradiation [10,11]. The variation of the inverse of the lifetime in epitaxial n-type GaAs is linear with the irradiation fluence

$$\tau^{-1} = \delta\varphi, \tag{1}$$

which is consistent with the fact that the introduced defects are primary defects, i.e. have a concentration proportional to the fluence. From the value of δ ($1.3 \times 10^{-7} \, \text{cm}^2 \, \text{s}^{-1}$ for 1 MeV electrons), we deduce a minority carrier cross section

$$\sigma_p = \delta/vv \tag{2}$$

(v is the thermal velocity of the carriers) equal to $\sigma_p \approx 10^{-13} \, \text{cm}^2$, a value in agreement with that evaluated for the H_3 trap [7]. Hence, for a layer with a typical minority carrier lifetime of 10^{-8} s, a fluence of about $10^{16} \, \text{cm}^2$ reduces this lifetime by a factor 10.

In n-type materials the total concentration of all electron traps, which determine the compensation of the doping concentration, is of the order of $1 \, \text{cm}^{-1}$ at room temperature, i.e. when the shallow traps (labelled E1 and E2) are ionized [4]. So, for instance, a fluence of $10^{17} \, \text{cm}^{-2}$ is necessary to fully compensate a $10^{17} \, \text{cm}^{-3}$ doped material.

3.2. GaInP

There have been extensive studies of electron- induced defects in InP (for the last one, see Ref. [12]) and GaP (for a recent study, see Ref. [13]), but to our knowledge only one has been performed in GaInP [14]. This last study showed that four electron traps are introduced in n-type layers, providing a total introduction rate for compensating centers of the order of 0.5 cm^{-1}. This suggests that, unlike in GaAs, the defects are probably secondary defects. The trap labelled IE4, reported in Ref. [14], associated with an energy level located at 0.65 eV below the conduction band and characterized by an introduction rate of 0.4 cm^{-1}, could well be the lifetime killer owing to the location of its energy level ($\sigma_n = 2.5 \times 10^{-12}$ cm^2). The characterization of defects in p-type layers is under way [15]. Here we only present (see Section 6), few data related to the fluence dependences of the concentration of compensating centers and of the minority carrier lifetime.

3.3. Silicon

In Si, the vacancies (V) which are initially produced, are mobile around 100 K. As a result, the defects present at room temperature correspond to the interaction of V with impurities. Thus, oxygen, present in large concentration in Czochralski (Cz)-grown materials, induces the formation of V–O complexes called A centers; complexes of V with the doping impurities are the E centers; vacancies can also interact between themselves producing divacancies (V–V). Hence, in a slightly doped Cz material the main defect is the A center; in a slightly doped float-zone material (which contains very little oxygen), the main defect is V–V; as to the E centers their concentration increases with the doping concentration. The electrical characteristics of these defects are given in Table 1 [16–20]. These characteristics strongly suggest that V–V is the main recombination center and the E center the compensating center. Demonstration that the E center is indeed the compensating center in p-type Cz material is given in Fig. 1. This figure shows that the concentration of compensating centers N_C varies as

$$N_C = N_A[1 - \exp(-\beta\varphi)], \tag{3}$$

Table 1
Capture cross sections of the various defects introduced by irradiation in Si

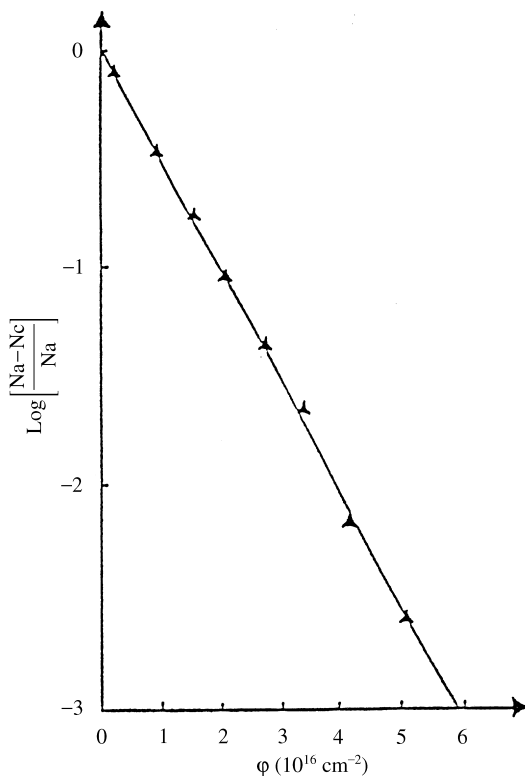|	A center	E center		Divacancy
	(V-O)	(V–D)	(V–A)	(V–V)
Level (eV)	$E_c - 0.17$	$E_c - 0.44$	$E_v + 0.18$	a: $E_c - 0.23$ $(2 - / -)$ b: $E_c - 0.39$ $(-/0)$ c: $E_v + 0.21$ $(0/+)$
Capture cross section (cm^2)	$\sigma_n = 10^{-14}$	$\sigma_n = 4 \times 10^{-15}$	$\sigma_n > 4 \times 10^{-16}$	$\sigma_{pc} = 10^{-17}$ $\sigma_{nc} = 4 \times 10^{-16}$ $\sigma_{na} = 10^{-16}$ $\sigma_{nb} = 10^{-15}$

Fig. 1. Variation of the concentration of compensating centers N_C in the p-type base of a Si cell doped at a level of 1.8×10^{15} cm^{-3}, introduced by a 1 MeV electron irradiation at room temperature. The variation is given under the logarithm form to show that N_C varies exponentially and saturates for the value of N_A. This demonstrates that the compensating centers are directly related to the doping impurity, i.e. are E centers.

where N_A is the doping concentration. It expresses the fact that N_C is proportional to the remaining fraction of the dopant impurities. As to the lifetime in Cz (p and n) materials following 10 MeV proton irradiation, it is characterized by $\delta = 5 \times 10^{-6}$ cm^2 s^{-1} [20–22]. With an introduction rate of 5×10^{-3} cm^{-1}, the cross section σ associated with the lifetime change is $\sigma \simeq 10^{-16}$ cm^2, a value compatible with the measured cross section for the divacancy.

4. Techniques of characterization

The information which is necessary to evaluate the cell degradation induced by a given irradiation, is
(i) the concentration N_C of the compensating centers, i.e. of the defects which compensate the doping concentration N_A;

(ii) the concentration N_R of the recombination centers, i.e. of the defects which induce minority carrier recombination;

(iii) the associated electron and hole capture cross sections (σ_n and σ_p) of the recombination centers. To these cross sections correspond the capture rates

$$\tau_{n,p} = (N_R v_{n,p} \sigma_{n,p})^{-1}, \tag{4}$$

where $v_{n,p}$ is the thermal velocity of the carriers. The minority carrier lifetime τ can be calculated directly from τ_n and τ_p.

Lifetime measurements provide the product $N_R \sigma_{n,p}$. These measurements can be performed using a variety of methods. The methods based on the use of a junction are of course best adapted since they can be directly applied on the solar cell itself. The most straightforward method consists to measure the current–voltage characteristics in dark (see, for instance, Ref. [21]). Extrapolation of the $\log I$ versus V plot to $V = 0$ provides values I_{01} and I_{02} which are respectively proportional to $\sqrt{\tau_n \tau_p}$ in the recombination regime (recognized by its slope $e/2kT$) and to τ in the diffusion regime (slope e/kT). Not only this technique is simple, but the magnitude of the signal increases when the lifetime decreases, which makes that the shortest the lifetime, the largest the signal.

The concentrations of any defect can in principle be measured using DLTS. However, in the DLTS conditions of measurement, all defects behave as majority or minority carrier traps, i.e. it is not possible to select which of the detected traps are recombination centers. Hence, the way to make this selection is to look for a linear relationship between the concentration N_i of each detected trap i versus I_{01} or I_{02}, as is illustrated in Fig. 2. DLTS allows also to evaluate the order of magnitude of the capture cross sections associated with majority (minority) carriers of majority (minority) carrier traps, but it cannot evaluate the minority carrier cross section of majority carrier traps.

As to the total concentration N_C of all compensating centers, it can be obtained by capacitance-voltage (C–V) measurements. The slope of the C^{-2} versus V plot is directly related to $N_A - N_C$ where N_A is the initial doping concentration of the material (see an illustration in Fig. 1).

In conclusion, it is possible to obtain all the parameters N_C, N_R, σ_n and σ_p needed to modelize the degradation of a cell by combining DLTS, I–V (in dark and under illumination) and C–V measurements. This will be illustrated in Section 6.

5. Mechanism of degradation

We illustrate the mechanism by which defects degrade a cell using the short circuit current, I_{SC}, induced by an illumination ϕ. The case of the open–circuit voltage which provides essentially the same information, is not developed here. The dark current being negligible under 0 V bias, the photocurrent I_{SC} is expressed as follows:

$$I_{SC} = e\phi \left[1 - \frac{\exp(-\alpha W)}{1 + \alpha L} \right], \tag{5}$$
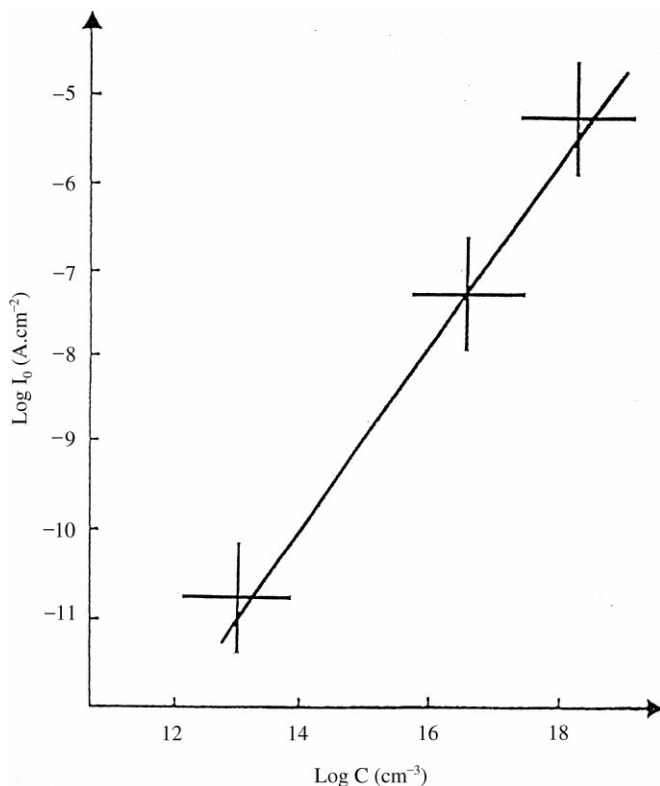
Fig. 2. Variation of the forward current extrapolated to 0 V, of junctions made of different n-type doped GaAs materials, versus the concentration C of the EL2 centers contained in these materials. The linear variation demonstrates that the recombination centers in GaAs are the EL2 defects, defects associated with As antisites.

where α is the absorption coefficient of the light, W the width of the space-charge region denoted by

$$W = \sqrt{\frac{2\varepsilon V_d}{e(N_A - N_C)}} \qquad (6)$$

and L the diffusion length by

$$L = \sqrt{D\tau} \qquad (7)$$

(D is the minority carrier diffusion length, ε is the dielectric constant, and V_d the built-in voltage).

Hence the degradation of I_{SC} occurs via the introduction of

(i) recombination centers which decrease τ, from the unirradiated value τ_0 to τ such that

$$1/\tau = 1/\tau_0 + 1/\tau_i, \qquad (8)$$

where τ_i is the lifetime associated with the irradiation-induced recombination centers,

(ii) compensating centers which decrease N_A and hence increase W.

In practice, the variation of I_{SC} versus the fluence φ can be divided into several ranges depending on the concentration of N_C and N_R (see Fig. 3):

(a) *Very low fluence*: N_C is small compared to N_A and N_R is small enough, so that τ_i remains larger than τ_0. There is no dependence of I_{SC} versus φ, until a critical fluence φ_C.

(b) *Low fluence*: N_C remains small compared to N_A but N_R has increased so that τ_i overcomes τ_0. I_{SC} decreases accordingly. As it will be shown in the next section, I_{SC} decreases approximatively linearly with $\log \varphi$.

(c) *Large fluence*: N_R is now so large that αL is smaller than one so that I_{SC}, given by relation (5), reduces to

$$I_{SC} = e\phi[1 - \exp(-\alpha W)]. \tag{9}$$

Then, I_{SC} increases with φ as a result of the increase of W due to the decrease of $N_A - N_C$.

(d) *Very large fluence*: I_{SC} drops to zero because of the abrupt change in the Fermi level position when a nearly complete compensation of the free carriers is reached, or when the material has changed its type.

From the variation of I_{SC} versus $\log \varphi$, in conjunction with the $I-V$ and $C-V$ characteristics, it is possible to extract all the necessary parameters. The $I-V$ characteristics in dark provide $\tau(0)$ and $\tau(\varphi)$, the $C-V$ characteristics provide $N_A-N_C(\varphi)$, from
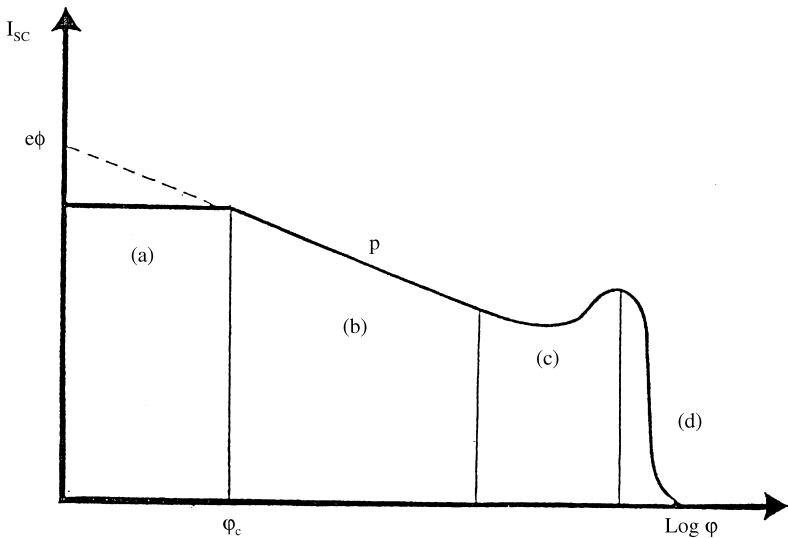

Fig. 3. Schematic representation of the variation of the short-circuit current versus the fluence of irradiation.

which $W(\varphi)$ is deduced. Then $I_{SC}(\log \varphi)$ allows to obtain $e\phi$ by extrapolation of $I_{SC}(\log \varphi)$ to $\log \varphi = 0$, and to calculate α from $I_{SC}(0)$, $W(0)$ and $L(0)$. In the range where I_{SC} decreases linearly versus $\log \varphi$, the quantity $\exp(-\alpha W)$ remains constant. The $I_{SC}(\varphi)$ dependence is only due to $L(\varphi)$, from which $\tau(\varphi)$ is derived. In range of large fluence, $\alpha L(\varphi)$ is negligible compared to 1 and the change in I_{SC} is only accounted for by that of $W(\varphi)$. Finally, when $N_A - N_C(\varphi)$ approaches to zero, I_{SC} drops to zero. These mechanisms of degradation are illustrated quantitatively in the next section.

6. Illustration: degradation of Si, GaAs and GaInP cells

The degradation data for Si, GaAs and GaInP cells induced by electron irradiation are presented in Table 2. They are deduced from Fig. 4 which represents the variations of the short-circuit currents $I_{SC}(\varphi)$, normalized to the unirradiated values $I_{SC}(0)$, versus the logarithm of the fluence φ. They correspond to cells illuminated with 0.1 AMO and irradiated at room temperature. These data describe also high fluence effects, to complement the preliminary studies of Refs. [23–26].

Si cells appear to be the most sensitive to irradiation (φ_C is the lowest) because the initial lifetime is the largest. It is therefore affected by less introduced recombination centers than in the case where the lifetime is shorter, i.e. the initial concentration of recombination centers larger.

For low fluences, the drop of I_{SC} for a given decade of fluence is also larger in Si than in GaAs and GaInP. This implies that the recombination centers introduced for a given fluence are in larger concentration, or more effective. However, for large fluences, I_{SC} for of GaAs and GaInP cells decreases faster than that for Si cells because the base doping is higher. Hence Si cells are less resistant than GaAs and GaInP cells at low fluences but this becomes the contrary at high fluences.

7. Conclusion

The understanding on the mechanisms by which defects induce the degradation of solar cells is correctly understood. Si and GaAs cells are well-mastered devices, for which a reasonable knowledge of the defects induced by proton and electron irradiations has been reached. It is therefore possible to predict correctly the degradation induced by a given irradiation. This is not yet the case for GaInP cells.

Table 2

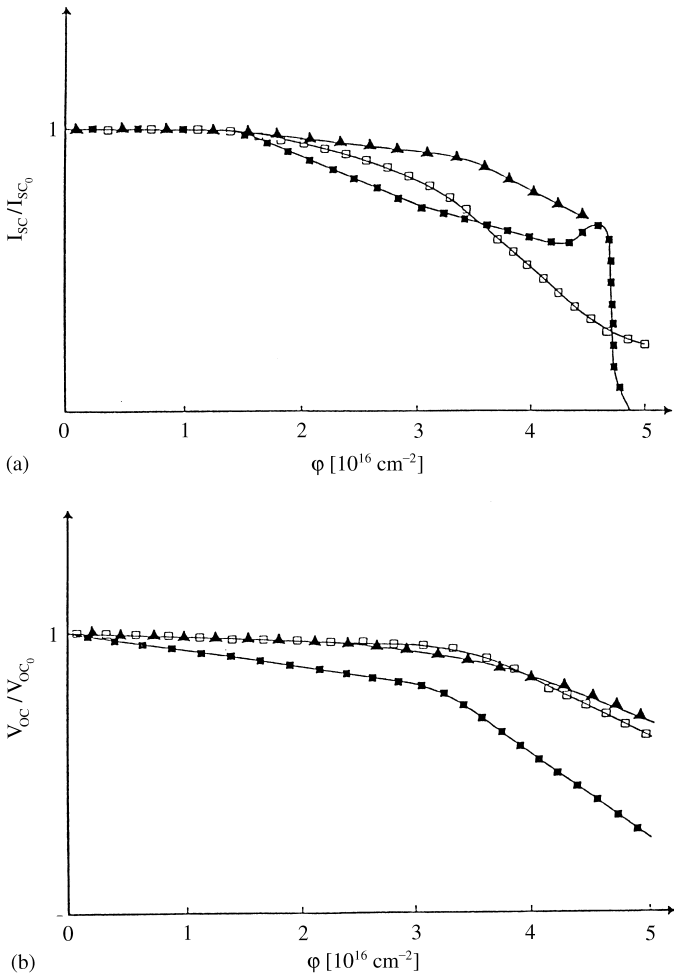| Cell	Type	Doping (cm^{-3})	τ_0 (s)	φ_0 (cm^{-2})	δ (cm^2 s^{-1})	β (cm^2)	v (cm^{-1})
Si	n$^+$–p	1.8×10^{15}	1×10^{-7}	2×10^{13}	4.5×10^{-9}	4.5×10^{-17}	
GaAs	p$^+$–n	6.7×10^{16}	5×10^{-10}	6×10^{13}	7×10^{-7}	—	0.18
GaInP	n$^+$–p	1.5×10^{17}	6×10^{-11}	5×10^{13}	6×10^{-7}	—	2.2

Fig. 4. Variations of the short-circuit current (a), and of the open–circuit voltage (b) normalized to the unirradiated values, measured under 0.1 AMO illumination at room temperature, versus the fluence of 1 MeV electron irradiation for Si (■), GaAs (□) and GaInP (▲) cells.

References

[1] J.W. Corbett, J.C. Bourgoin, Defects creation in semiconductors, in: J.H. Crawford, L.M. Slifkin (Eds.), Point Defects in Solids, Vol. 2, Plenum Press, New York, 1974 (Chapter 1).
[2] J.W. Corbett, Solid State Phys. (Suppl. 7) (1966) Chap. 3, p. 59.
[3] F.H. Eisen, K. Bachem, E. Klausman, K. Kœhler, R. Haddad, J. Appl. Phys. 72 (1992) 5593.
[4] D. Pons, J.C. Bourgoin, J. Phys. C 18 (1985) 3839.
[5] H.J. Lim, H.J. von Bardeleben, J.C. Bourgoin, J. Appl. Phys. 62 (1987) 2738.
[6] D. Stievenard, X. Boddaert, J.C. Bourgoin, H.J. von Bardeleben, Phys. Rev. B 41 (1990) 5271.
[7] D. Stievenard, X. Boddaert, J.C. Bourgoin, Phys. Rev. B 34 (1986) 4048.
[8] J.C. Bourgoin, K. Khirouni, M. Stellmacher, Appl. Phys. Lett. 72 (1998) 442.
[9] J.C. Bourgoin, H.J. von Bardeleben, D. Stievenard, J. Appl. Phys. 64 (1988) R65.
[10] R. Ferrini, M. Galli, G. Guizzetti, M. Patrini, F. Nava, C. Canali, P. Vanni, Appl. Phys. Lett. 71 (1997) 3084.
[11] H.J. von Bardeleben, J.C. Bourgoin, J. Appl. Phys. 58 (1985) 1041.
[12] A. Sibille, Phys. Rev. B 35 (1987) 3929.
[13] M.A. Zaidi, M. Zazoui, J.C. Bourgoin, J. Appl. Phys. 74 (1993) 4948.
[14] M.A. Zaidi, M. Zazoui, J.C. Bourgoin, J. Appl. Phys. 73 (1993) 7229.
[15] A. Khan, Y. Yamaguchi, T. Takamoto, N. de Angelis, J.C. Bourgoin, J. Cryst. Growth 210 (2000) 264.
[16] L.C. Kimerling, Inst. Phys. Conf. Ser. 31 (1977) 221.
[17] S.D. Brotherton, G.J. Parker, A. Gill, J. Appl. Phys. 54 (1983) 5112.
[18] A.O. Evwaraye, E. Sun, J. Appl. Phys. 47 (1976) 3776.
[19] M.W. Hüppi, J. Appl. Phys. 68 (1990) 2702.
[20] S.D. Brotherton, P. Bradley, J. Appl. Phys. 53 (1982) 5720.
[21] E. Simoen, J. Vanhellemont, C. Claeys, Appl. Phys. Lett. 69 (1996) 2858.
[22] A. Hallén, N. Keskitalo, F. Masszi, V. Nàgl, J. Appl. Phys. 79 (1996) 3906.
[23] M. Yamaguchi, S.J. Taylor, M.J. Yang, S. Matsuda, O. Kawasaki, T. Hisamatsu, J. Appl. Phys. 80 (1996) 4916.
[24] M. Imaizumi, S.J. Taylor, M. Yamaguchi, Proceedings of the 26th IEEE Photovoltaic Specialists Conference, Anaheim, CA, 1997, p. 983.
[25] S.J. Taylor, M. Yamaguchi, M. Imaizumi, M.J. Yang, T. Iko, T. Yamaguchi, S. Watanabe, K. Ando, Proceedings of the 26th IEEE Photovoltaic Specialists Conference, Anaheim, CA, 1997, p. 835.
[26] M. Yamaguchi, K. Ando, J. Appl. Phys. 63 (1988) 5555.